

# PKS 2351-154: a high-redshift quasar with variable X-ray absorption

N. Schartel<sup>1,2</sup>, S. Komossa<sup>3</sup>, W. Brinkmann<sup>3</sup>, H.H. Fink<sup>3</sup>, J. Trümper<sup>3</sup>, and W. Wamsteker<sup>1,2</sup>

<sup>1</sup> ESA, IUE Observatory, P.O. Box 50727, E-28080 Madrid, Spain

<sup>2</sup> Affiliated to the Astrophysics Division, Space Science Department, ESTEC

<sup>3</sup> Max-Planck-Institut für Extraterrestrische Physik, D-85740 Garching, Germany

Received 5 July 1996 / Accepted 20 August 1996

**Abstract.** The ROSAT PSPC spectrum of the high-redshift quasar PKS 2351-154 ( $z = 2.671$ ) shows absorption which is significantly larger than the Galactic value in the direction of the source. This absorption is variable on time scales of  $\leq 1.5$  years corresponding to 0.41 years in the quasar's rest frame. In addition, we find indications that absorbing material is located at high redshifts. Optical observations revealed a CIV system with  $z_{abs} \approx z_{em}$ . We conclude that this CIV system is related to the variable X-ray absorption. The variations can be explained in terms of changes in the ionization state of the absorbing material. In that case, the CIV system could be variable, too, and it could be close to the active galactic nucleus itself.

**Key words:** quasars: PKS 2351-154 – galaxies: ISM – X-rays: galaxies

---

## 1. Introduction

The investigation of the X-ray emission of high redshift quasars is important for two reasons: Firstly, because of the cosmological evolution of the X-ray spectra of quasars. For example, the ROSAT/PSPC spectral energy range of a quasar with  $z \approx 3$  corresponds to the 0.4 - 9.6 keV energy band in the quasar's rest frame. Therefore, the soft spectra of high redshift QSOs can be compared directly with observations of low redshift quasars observed by EXOSAT or Ginga. The second reason is the opportunity to study in the X-ray energy band absorption systems along the line of sight. This may help to understand the distribution of metal-rich absorbing systems at high redshifts.

Before ROSAT the X-ray study of quasars was restricted to low redshift sources as no spectra with sufficiently high photon statistics could be obtained from more distant objects. The high spatial resolution and sensitivity of ROSAT allows for the first

time a detailed study of X-ray spectra of high-redshift quasars ( $z > 2.0$ ). Because of the long exposures (typically some ten thousand seconds) required to obtain sufficient photon statistics in pointed ROSAT/PSPC observations, the number of X-ray spectra of high redshift quasars is still rather small. So far X-ray spectra of five high redshift quasars with good photon statistics (net counts  $> 300$ ) have been published. One of the exciting results was the detection of absorption in excess of the Galactic value (Wilkes et al., 1992): PKS 0483-436 ( $z = 2.85$ ) shows excess absorption of  $N_H = 8.6^{+4.4}_{-2.8} \times 10^{21} \text{ cm}^{-2}$  assuming that the absorption is located at the quasar (Wilkes et al., 1992, Elvis et al., 1994). On the other hand, the ASCA spectrum of PKS 2126-158 ( $z = 3.275$ ) indicates that the excess absorption detected is located close to our own galaxy (Elvis et al., 1994, and Serlemitsos et al., 1994). The other three published high redshift quasars show either no excess absorption (Q 1745+624 with  $z = 3.87$  (Fink and Briel, 1993) and Q 0420-388 with  $z = 3.12$  (Elvis et al., 1994), or a possible excess absorption cannot be detected due to a high Galactic absorbing column density (S5 0014+813, Elvis et al., 1994).

## 2. Observation and analysis

Only a relatively small number of high-redshift quasars were detected in the ROSAT All Sky Survey (hereafter RASS) by means of positional coincidences (Brinkmann, 1992). From them we selected the radio-loud quasar PKS 2351-154 as a target for a pointed observation because of an expected high count rate and a low Galactic column density of  $N_H = 2.18 \pm 0.26 \times 10^{20} \text{ cm}^{-2}$  (Stark et al., 1992).

The ROSAT/PSPC observations were performed with the source in the center of the detector field. Table 1 gives the log and the accumulated photon collection times of the two observations which are separated by  $\approx 1.5$  years. The source counts were extracted from a circle of 2.0' radius centered on the X-ray position. Using this radius at the center of the detector field, we extracted more than 99 per cent of the source counts. The back-

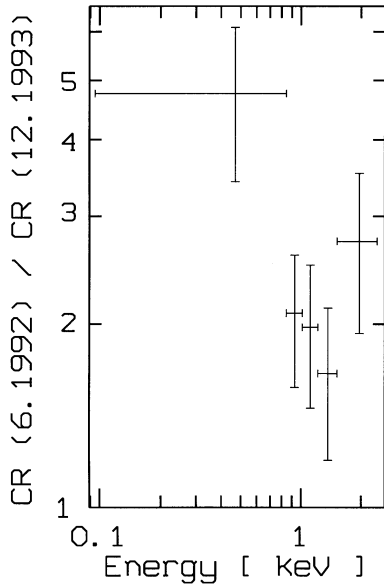


**Fig. 1.** The large spectral variability is shown by the ratio between the count rate of the first observation and that of the second observation versus energy in five energy bins. Both count rates were corrected for vignetting as well as for dead time effects.

ground was determined from an annulus of inner radius of  $3'$  and outer radius of  $10'$ , from which all sources detected with a likelihood greater than 10 were removed. The limit corresponds to a  $4\sigma$ -detection. Each count of the background was corrected individually for vignetting. The dead time corrected count rates in the PSPC channels 10 through 240 (0.1 - 2.4 keV) for the two observations are given in Table 1, too. These channels correspond to the 0.37 - 8.8 keV energy band in the quasar's rest frame. The count rates differ by a factor of  $2.7 \pm 0.3$  in the two pointings. Such a variation is not unusual for AGN in the analyzed energy band. The study of the medium energy spectra (2.0 - 6.0 keV) of the complete hard X-ray selected Piccinotti AGN sample established evidence for variability in almost all sources (Grandi et al., 1992) and variations of up to a factor of five were found in the medium energy range.

The spectral and intensity variations observed in PKS 2351-154 are rather unusual. Fig. 1 shows the ratio between the count rate of the first and the second observation plotted as a function of energy. Due to the low number of counts in the current observations we show the high significance of the spectral variation by calculating a hardness ratio, defined as  $HR = (Hard - Soft)/(Soft + Hard)$ . We defined the soft band from channel 10 through 79 and the hard band from channels 80 through 240. In the quasar's rest frame these energy bands correspond to 0.4 - 2.9 keV for the soft and to 2.9 - 8.8 keV for the hard band, respectively. In Table 1 we give the background-corrected count rates for the two energy bands and the resulting hardness ratios. The two X-ray spectra of PKS 2351-154 show a significant difference in the hardness ratios,  $\Delta HR = 0.38 \pm 0.09$ , and, thus a significant spectral variation. The time lapse of about 1.5 years between the two measure-

**Table 1.** Log of the ROSAT Observations

Observation:	1 <sup>st</sup>	2 <sup>nd</sup>
Start (Date)	Jun 06, 1992	Dec 13, 1993
Start (UT)	18:00:21	21:31:01
End (Date)	19.06.1992	14.12.1993
End (UT)	19:54:13	11:14:18
Accepted time (sec)	6335	12808
Count rate <sup>(a)(b)</sup>	$69.5 \pm 3.7$	$25.3 \pm 1.8$
Soft count rate <sup>(a)(c)</sup>	$27.6 \pm 2.6$	$5.3 \pm 1.2$
Hard count rate <sup>(a)(d)</sup>	$41.9 \pm 2.7$	$20.0 \pm 1.3$
Hardness ratio	$0.20 \pm 0.05$	$0.58 \pm 0.08$

(a): corrected for vignetting and for dead time in  $10^{-3} \text{ s}^{-1}$

(b): for channels 10 through 240

(c): for channel 10 through 79

(d): for channel 80 through 240

ments limits the origin of the spectral variability to an emission volume with diameter of about 0.4 light years. In the second observation we find almost no flux in the 0.4 - 2.9 keV energy band in the quasar's rest frame (see first energy bin in Fig. 1). Therefore, either there are dramatic intrinsic changes in the soft part of the quasar's X-ray spectrum or the spectral variability must be caused by a drastic change in the absorbing column density.

To derive physical parameters describing the X-ray emission of PKS 2351-154 we fitted simple spectral models to the data. We binned the pulse height spectra such that each bin is characterized by a signal to noise ratio greater than five. We used the PSPC detector response matrix version 11.03.1995; however, tests with other versions of the response matrix yielded results which are consistent within the statistical uncertainties. The results of the fits are provided in table 2. The given errors correspond to the 68% and the 90% confidence level for one interesting parameter, respectively.

A simple power law model with absorption fixed at the Galactic value using the cross sections by Morrison and McCammon (1983) is unlikely for the first observation ( $\chi^2 = 9.54$  with  $d.o.f = 7$ ) and ruled out for the second observation ( $\chi^2 = 20.87$  with  $d.o.f = 6$ ) as the reduced  $\chi^2$  value is unacceptable. In addition, the derived photon indices for both observations of  $\Gamma = 1.32$  and  $\Gamma = 0.91$  would have been rather unusual for quasars in this energy band (0.3 - 8.8 keV in the quasar's rest frame). In order to estimate the amount of excess absorbing column density, we used the same model but left the absorbing column density free to vary (Fit 1). The two dimensional confidence contours (68.3%, 90.0%, 95.4%) in the  $N_H - \Gamma$  phase space are plotted in Fig. 2. The contours of the two observations are marked by their date. In both observations we find an absorbing column density significantly larger than the Galactic value. Considering the photon index and the intrinsic absorption it is evident that the X-ray spectrum of the first observation shows no

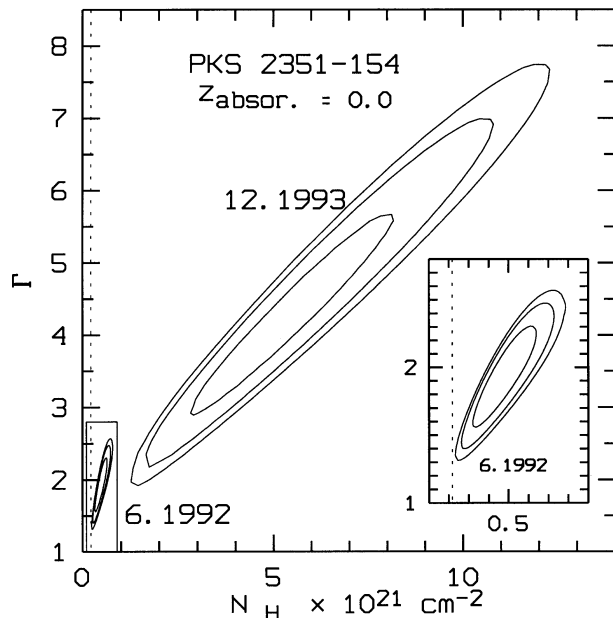


**Fig. 2.** Two dimensional contours for 68.3%, 90.0%, and 95.4% confidence levels are given assuming that the absorbing material is located at  $z = 0.0$ . The two observations are characterized by their date. The dotted line indicates the Galactic column density. For clarity, the confidence contours of the first observation are given in the insert again, on a larger scale.

soft excess emission, as is very common in low redshift ROSAT quasar spectra (see for example Schartel et al. 1996). Therefore, it seems unlikely that a variable soft excess is the origin of the spectral variations found. Because of the poor photon statistics of the second observation, in combination with the large energy range covered by the first bin, we cannot determine the photon index in the second observation very well. In particular, we cannot decide whether the steepness of the spectral slope is created by the low photon statistics or whether it is an indication for a more complex emission mechanism. As the absorbing column density and spectral index are not independent of each other we fitted the spectrum of the second observation by fixing the photon index at  $\Gamma = 1.92$ , the value obtained from the first observation (Fit 2). We obtained an absorbing column density of  $N_{H(z=0.0)} = 1.27^{+0.37}_{-0.29} \times 10^{21} \text{ cm}^{-2}$  which, again, is clearly in excess of the Galactic value.

As the short variability time scale strongly suggests that the excess column density is located near the active nucleus, we performed power law fits assuming that the absorber is located at  $z = 2.6775$  (see next section). Within the uncertainties we obtain the same photon indices as in Fit 2 for both observations. Modeling the second observation again with a fixed power law (Fit 4) we obtained an intrinsic absorption of  $N_{H(z=2.6775)} = 2.0^{+0.9}_{-0.6} \times 10^{22} \text{ cm}^{-2}$ . The pulse height spectra and the best fits are plotted in Fig. 3.

In order to assess whether the data can also be described in terms of warm absorption, we calculated a sequence of warm absorber models using the code *Cloudy* (Ferland 1993). We

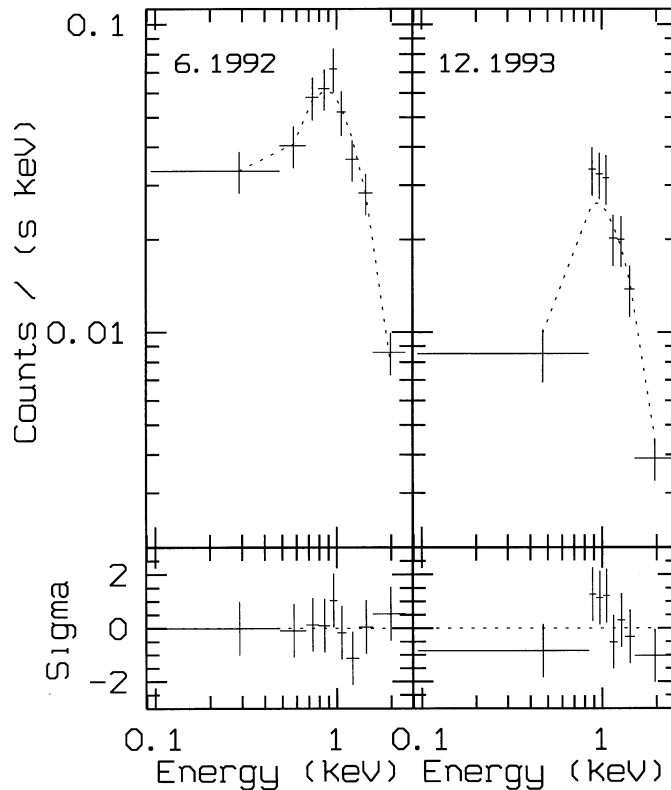


**Fig. 3.** ROSAT PSPC pulse height spectra for the two observations of PKS 2351-154. The first upper panel shows the pulse height spectrum of the June 1992 observation and the best fit power-law plus cold absorption at  $z=2.6775$  in addition to the fixed Galactic one. The second upper panel shows the spectrum for the December 1993 observation and the best fit power-law plus absorption at  $z=2.6775$  in addition to the fixed Galactic one. Here the power-law index was fixed to 1.9, which was obtained for the fit of the spectrum of the first observation. The lower panel shows the residuals from these fits.

stress, that no detailed modeling has been attempted, due to the low number of photons in the current observations. The spectral energy distribution (SED) incident on the warm gas was assumed to originate from the point-like central energy source of the quasar. The SED chosen for the modeling consists of an UV-EUV power law with a energy index  $\alpha_{uv-x}=1.4$  extending up to 0.1 keV, an intrinsic X-ray power law with  $\Gamma_x=1.9$  and a mean continuum after Padovani and Rafanelli (1988) from the radio to the optical region with a break at  $10\mu\text{m}$  and an energy index  $\alpha=2.5$  longward of  $\lambda = 10\mu\text{m}$ . The ionization state of the warm absorber can be described by the warm hydrogen column density  $N_w$  and the ionization parameter  $U$ , defined as  $U = Q/(4\pi r^2 n_H c)$ , where  $Q$  is the number rate of photons above the Lyman limit,  $r$  is the distance between the nucleus and the warm absorber,  $n_H$  is the hydrogen density (fixed to  $10^{9.5} \text{ cm}^{-3}$ ) and  $c$  the speed of light. The lowest value of  $U$  considered in the models is  $\log U = -2.0$ . For values lower than that, the absorber starts getting ‘cold’. Solar abundances (Grevesse and Anders 1989) were adopted. A cold absorbing column corresponding to the Galactic value was added.

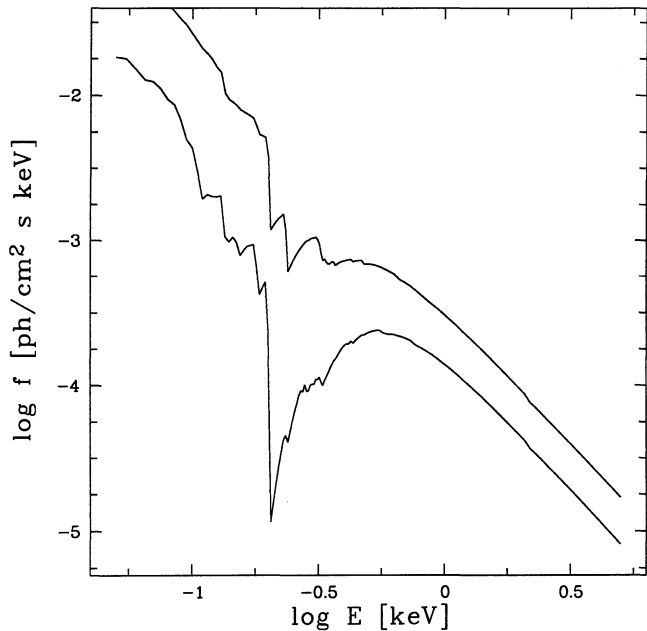


**Fig. 4.** Defolded warm absorbed X-ray spectra for both observations corrected for Galactic cold absorption (the upper one corresponds to the first observation). The change in the absorption structure is due to a factor of 2 decrease in the ionization parameter.

In a first step, we determined  $U$  and  $N_w$  independently for both observations. We find that the warm absorber model is able to reproduce the observations successfully. However, due to the rather low number of photons available, a range of  $U, N_w$  pairs fits the data equally well. For the first observation, we find best-fit parameters of  $(\log U, \log N_w) = (-0.6, 21.9)$  and an observed flux at 10 keV  $f_{10}$  of  $10^{-5.38}$  ph cm $^{-2}$  s $^{-1}$  keV $^{-1}$ , with  $\chi^2_{\text{red}} = 0.82$ . Models are also acceptable statistically with  $(-2.0, 21.6)$  or  $(0.05, 22.4)$  and intermediate values, with  $\chi^2_{\text{red}} \leq 1.1$ . The corresponding range of successful warm absorber models for the second observation is  $(\log U, \log N_w) = (-2.0, 22.2)$  to  $(-0.2, 22.5)$ .

In a second step, we tested whether both observations can be described by a change in the ionization parameter only, according to the observed drop in luminosity by about a factor of 2. We find that this is possible for warm column densities around  $\log N_w = 22.4$ . Fixing  $N_w$  to this value results in an ionization parameter of  $\log U = 0.05$  for the first observation and a flux of  $\log f_{10} = -5.34$ . Within the uncertainties, the same model, but with  $\log U = -0.25$  and  $\log f_{10} = -5.67$ , can describe the second observation. Although an additional change in the warm column density cannot be excluded with the present data, in the following discussion we only refer to the second model with constant  $N_w$ .

The column densities of some ions expected to show up as UV absorbers are  $\log N_{\text{C}^{3+}} = 15.2$ ,  $\log N_{\text{N}^{4+}} = 14.8$  and  $\log N_{\text{H}^0} = 16.2$  for the model describing the first observation, and  $\log N_{\text{C}^{3+}} = 17.2$ ,  $\log N_{\text{N}^{4+}} = 16.6$  and  $\log N_{\text{H}^0} = 16.9$  for the second observation. In both models, silicon is highly ionized, with negligible abundances of  $\text{Si}^{2+}$  and  $\text{Si}^{3+}$ . In order to explicitly decide

whether the optical -UV - X-ray absorber is one and the same (an approach developed by Mathur et al.; e.g. Mathur, 1994, Mathur et al., 1994), simultaneous observations in both energy ranges are needed, given the observed variability of the absorption features.

### 3. Optical observations

The quasar was studied spectroscopically by Roberts et al. (1978) with  $\approx 1.5\text{\AA}$  resolution and a spectral coverage from 3600 to 5000  $\text{\AA}$ . Besides different absorbing systems classified as 'probable' or 'possible', they found a metal line system labeled as 'certain' at  $z \approx 2.6775$  with the following ions in absorption: HI with a rest wavelength of 1215.7  $\text{\AA}$ , CIV (at 1548.2  $\text{\AA}$  and at 1550.8  $\text{\AA}$ ), SiIII (at 1206.5  $\text{\AA}$ ) and SiIV (at 1393.8  $\text{\AA}$  and at 1402.8  $\text{\AA}$ ). In 1988 PKS 2351-154 was again the target of an optical study using a resolution of about 5 $\text{\AA}$ . The blue spectra cover a wavelength range of approximately 3880 - 5560  $\text{\AA}$  while the red spectra overlap covering 5500 - 7760  $\text{\AA}$ . In the obtained spectra the lines of SiIV and CIV are not conspicuous (Barthel et al., 1990). Although the optical spectra are difficult to compare because of the different spectral resolution, it seems that the HI equivalent width is a factor 2-3 larger in the spectra taken by Barthel.

Most CIV absorption systems found in quasar spectra are intervening at cosmological distances from the quasar, as they are randomly distributed in redshift at  $z_{\text{abs}} < z_{\text{em}}$  (see for example Weymann et al., 1981). The existence of a peak in the redshift distribution of CIV absorption systems at  $z_{\text{abs}} \approx z_{\text{em}}$  was first claimed by Weymann et al. (1979) and confirmed in the samples discussed by Foltz et al. (1986), and Anderson et al. (1987). However, Young et al. (1982) and Sargent et al. (1989) did not find an excess of such systems in their quasar samples. As all samples are large enough for the differences to be statistically significant, Foltz et al. (1986) and Anderson et al. (1987) assumed that the differences are related to the radio properties of the quasars, whereas Möller and Jakobson (1987) assume them to be due to both the quasars' optical and radio luminosity.

### 4. Results, interpretation, and discussion

The X-ray spectrum obtained in the first observation is characterized by the "canonical" power law index and absorption in excess of the Galactic value. High resolution optical spectroscopy provides as a candidate for the excess absorption a CIV system with  $z_{\text{abs}} \approx z_{\text{em}}$ .

Unfortunately, the poor photon statistics of the second observation in combination with the large energy range covered by the first spectral bin does not allow to fit more complex models to that spectrum. However, Fig. 1 clearly demonstrates that the spectral variability in the object is significant. In the second observation the absorption is in excess of the Galactic value and significantly higher than in the first observation. The variability is a strong indication that the absorption system is located near the active galactic nucleus and could therefore be associated

with the CIV system found in the optical observation. According to EXOSAT and *Ginga* observations of low redshift quasars and according to the photon indices obtained for ROSAT observations of high redshift quasars, it appears unlikely that the quasar has changed its spectral slope from  $\Gamma = 1.8$  to  $\Gamma = 3.4$ , the only other viable explanation.

The variability limits the area covered by the absorbing material to a typical size of  $\approx 0.4$  light years, assuming it to be located at  $z_{Quasar} = 2.6710$ . On the other hand, as there is no significant flux below 0.67 keV, the absorbing material must completely cover the X-ray emitting area of the galactic nucleus. The X-ray absorption in this energy range (in the quasar's rest frame) is a direct measurement of the K-edge strengths' of metals. The optically detected elements (C and Si) demonstrate that the CIV system indeed provides the elements necessary to explain the X-ray absorption features. Further, the detected lines of CIV, SiIII, and SiIV show that at last a part of the absorbing material is ionized. Because the CIV system is seen in two optical studies obtained of approximately 10 years apart we have a lower limit for its lifetime of 2.7 years in its rest frame. If the X-ray absorber is identical with the CIV system then the lifetime increases to more than 4.1 years. There are three possible scenarios which are, however, indistinguishable by our analysis:

The first scenario are clouds with a typical size larger than the X-ray emitting region of the quasar surrounding the active nucleus. These clouds show different absorbing column densities as well as different ionization levels. In this scenario we have to consider that a different cloud is responsible for the rapid variability of the X-ray absorption which is not identical with the found CIV system. On the other hand the lifetime found for the CIV system in the optical is already 7 times larger than the time delay between the two X-ray observations whereas the time between the X-ray observations and the optical study of Bathels is only half of the time delay between his study and the earlier observations of Roberts. Therefore, it seems more likely that indeed the CIV system is the absorbing system in all four observations.

The second possible scenario is the interaction of a jet with a cloud of size smaller than the 0.4 light years where the jet changes the ionization level of the material in the cloud.

The third and most likely scenario was proposed to explain the variable X-ray absorption of the low redshift quasars MR 2251-178 (Halpern, 1984; Pan, Stewart & Pounds, 1990) and NRAO 140 (Marscher, 1988). According to this the active nucleus is embedded in absorbing material which changes the absorption as a function of the ionization level (warm absorber). During the first observation the X-ray flux found in the 0.8 - 2.4 keV energy range (corresponding to the 2.9 - 8.8 keV band in the systems rest frame) was  $0.042 \pm 0.003$  photons  $s^{-1}$ . In the second we found only  $0.020 \pm 0.001$  photons  $s^{-1}$ . As the flux decreases, the material around the source becomes less ionized and therefore less transparent. We have shown in Sect. 2 that a consistent description of the data is possible for a warm column density of  $N_w \approx \log 22.4$  with a drop in ionization parameter (from  $\log U \approx 0.05$  in the first observation to  $\log U \approx -0.25$  in the second) by the same factor of 2 as in the lumi-

**Table 2.** PKS 2351-154: spectral analysis

Observation:	1 <sup>st</sup>	2 <sup>nd</sup>
Fit 1:		
$N_H^{(a)}$ ( $z=0.0$ )	$0.46^{+0.11/+0.20}_{-0.10/-0.16}$	$4.9^{+2.7/+4.7}_{-2.1/-3.2}$
$\Gamma$	$1.9^{+0.3/+0.4}_{-0.2/-0.4}$	$4.0^{+0.3/+0.5}_{-0.3/-0.5}$
$F_{(0.1-2.4\text{keV})}^{(b)}$	$9.9^{+2.6/+5.0}_{-1.7/-2.5}$	$268^{+7103./+111426.}_{-243./-259.}$
$\chi^2 / d.o.f.$	2.74 / 6	3.31 / 5
Fit 2:		
$N_H^{(a)}$ ( $z=0.0$ )		$1.3^{+0.4/+0.6}_{-0.3/-0.4}$
$\Gamma$		$1.9^{(c)}$
$F_{(0.1-2.4\text{keV})}^{(b)}$		$5.3^{+0.6/+0.9}_{-0.5/-0.8}$
$\chi^2 / d.o.f.$		7.72 / 6
Fit 3:		
$N_H^{(a)}$ gal.	$0.218^{(c)}$	$0.218^{(c)}$
$N_H^{(a)}$ ( $z=2.6775$ )	$3.7^{+1.6/+2.7}_{-1.5/-2.4}$	$76^{+47./+85.}_{-35./-52.}$
$\Gamma$	$1.9^{+0.2/+0.4}_{-0.2/-0.4}$	$3.4^{+1.0/+2.3}_{-0.8/-1.3}$
$F_{(0.1-2.4\text{keV})}^{(b)}$	$8.2^{+5.2/+11.}_{-2.9/-4.3}$	$409^{+18081/+325000}_{-379/-397}$
$\chi^2 / d.o.f.$	2.68 / 6	2.66 / 5
Fit 4:		
$N_H^{(a)}$ gal.		$0.218^{(c)}$
$N_H^{(a)}$ ( $z=2.655$ )		$20^{+9/+15}_{-6/-9}$
$\Gamma$		$1.9^{(c)}$
$F_{(0.1-2.4\text{keV})}^{(b)}$		$4.3^{+0.4/+0.8}_{-0.4/-0.6}$
$\chi^2 / d.o.f.$		6.56 / 6

(a): in  $10^{21} \text{cm}^{-2}$  (c): fixed

(b): in  $10^{-4} \text{keVcm}^{-2} \text{s}^{-1}$

osity. This corresponds to a change in the HI column density from  $N_{HI} = 1.6 \times 10^{16} \text{cm}^{-2}$  to  $N_{HI} = 7.9 \times 10^{16} \text{cm}^{-2}$ . The strongest line seen in both optical observations, and the only one to allow a determination of the column density in both cases, is Ly  $\alpha$ . Assuming  $b = 60 \text{km/s}$  for the mean velocity dispersion we obtain for the first optical observation  $N_{HI} = 2.5 \times 10^{14} - 1.5 \times 10^{16} \text{cm}^{-2}$  and for the second  $N_{HI} = 3.2 \times 10^{18} \text{cm}^{-2}$ , respectively. According to the large uncertainties in the X-ray spectral fits, which is caused by the low number of photons, and according to the observed variability, the derived  $N_{HI}$ -values for the optical observations and for the X-ray observations are compatible.

A lower limit on the distance  $d$  of the absorber from the nucleus results from the fact that it covers the broad emission lines, which places the material outside the broad line region. An upper limit for the location of the absorber can be estimated

**Table 3.** PKS 2351-154: Radio measurements

$\nu$ [GHz]	$S_\nu$ [Jy]	Reference
0.365	$1.175 \pm 0.04$	Douglas et al., 1996
0.408	$1.14 \pm 0.05$	Large et al., 1991,
1.415	$0.8 \pm 0.2$	Ehman et al., 1970, and Rinsland et al. 1974
1.400	$0.838 \pm 0.025$	NARO VLA Sky Survey, Condon et al., 1996
2.700	$1.08 \pm 0.037$	Otrupcek and Wright, 1990
4.850	$0.97 \pm 0.052$	Griffith et al. 1994,
5.000	$0.93 \pm 0.020$	Otrupcek and Wright 1990
8.400	$0.78 \pm 0.062$	Wright et al. 1991
31.4	$0.56 \pm 0.11$	Geldzahler and Witzel, 1981

within the framework of the warm absorber scenario: The warm material reacts to a drop in the ionizing luminosity within its recombination time scale, which is less than 0.4 years in the present observations and is given by  $t_{\text{rec}} \approx \frac{1}{n_e} \frac{n_i}{n_{i+1}} \frac{1}{\alpha_{i+1,i}}$  where  $n_i/n_{i+1}$  is the abundance ratio of the metal ions dominating the cooling of the gas,  $\alpha_{i+1,i}$  is the corresponding recombination rate coefficient (Steenberg, 1982) and  $n_e$  the electron density. With an oxygen ion abundance ratio of  $n_{\text{O}^{6+}}/n_{\text{O}^{7+}} \approx 0.5$ , a recombination rate coefficient of  $\alpha = 1.3 \times 10^{-11} \text{ cm}^3/\text{s}$  (Shull & Van Steenberg, 1982) and  $t_{\text{rec}} \leq 0.4 \text{ y}$  this translates to a lower limit on the density of the absorber of  $n \geq 5 \times 10^3 \text{ cm}^{-3}$ . The defining equation of  $U$  than yields an upper limit for the location of the ionized material of  $d \leq 1 \text{ kpc}$ . The difference in redshift between emission ( $z = 2.6710$ ) and absorption ( $z = 2.6775$ ) lines suggests the material is infalling with a velocity of  $\approx 2000 \text{ km/s}$ .

The two other high-redshift quasars with intrinsic absorption, PKS 0438-436 and PKS 2126-158, are also radio-loud and show Giga-Hertz-peaked spectra. Therefore, Elvis et al. (1994) suggested that X-ray absorption may be caused by cold material in the intracluster gas around the quasar, for example a cooling flow. Through either free-free absorption or synchrotron self-absorption this material can cause the Giga-Hertz-peaked radio spectrum, due to the increased compactness. The radio data available (see Table 3) show PKS 2351-154 to have a flat spectrum ( $s \sim \nu^{-0.05}$ ) from 0.365 to 1.4 GHz and a slightly steeper one between 1.4 and 8.4 GHz ( $s \sim \nu^{-0.32}$ ), but no indication of a turnover at low frequencies. The absence of absorption towards Q0420-388, although it is a candidate Giga-Hertz-peaked quasar (Elvis et al., 1994), demonstrates that absorption is most probably not a universal characteristic of Giga-Hertz-peaked quasars. On the other hand due to the low number of studied high redshift quasars in the X-ray the results obtained of PKS 2351-154 demonstrate that absorption is maybe also common

in high redshift radio-loud quasars, independent of special radio features.

The combination of the results obtained from the analysis of the X-ray spectra together with the optical observations strongly suggests that the CIV system at  $z_{\text{abs}} \approx z_{\text{em}}$  is variable in time and belongs to the nearest environment of the active galactic nucleus itself. Optical observation of such systems in combination with ultraviolet and X-ray observations provide a powerful tool to study the material in the local environment of active nuclei even in high redshift objects.

*Acknowledgements.* The ROSAT mission is supported by the Bundesministerium für Bildung, Wissenschaft, Forschung und Technologie, BMBF, and by the Max-Planck-Gesellschaft. We thank the SASS team for processing the data and the EXSAS team for providing a software package for the reduction of the ROSAT data. We thank P. Barthel for supplying his optical spectrum and H. Andernach, P. Rodríguez, and our referee, B. Wilkes, for fruitful discussion and helpful comments. This research has benefitted from the radio data provided by the "Einstein On-line Service (EOLS)" maintained at Center for Astrophysics, Cambridge, MA.

## References

- Anderson S. F., Weyman R. J., Foltz C. B., Chaffee Jr F. H., 1987, *Astron. J.*, **94**, 278
- Barthel P. D., Tytler, D. R., Thomson B., 1990, *A&A Suppl. Ser.* **82**, 339
- Brinkmann W., 1992, in *X-Ray Emission from Active Galactic Nuclei and the Cosmic X-Ray Background*, ed. by Brinkmann W. and Trümper J., MPE Report 235, p.143
- Condon J. J., Cotton W. D., Greisen E. W., Yin Q. F., Perley R. A., Broderick J. J., submitted to *AJ*
- Douglas J. N., Bash, F. N., & Wolfe, C., 1996, *AJ* **111**, 1945
- Ehman J. R., Dixon R. S., & Kraus J. D., 1970, *AJ* **75**, 351
- Elvis M., Fiore F., Wilkes B. J., McDowell J. C., Bechtold J., 1994, *ApJ* **422**, 60
- Ferland G.J., 1993, University of Kentucky, Physics Department, Internal Report
- Fink H. H., Briel U. G., 1993, *A&A* **274**, L45
- Foltz C. B., Weymann R. J., Peterson B. M., Sun L., Malkan M. A., Chaffee F. H. Jr., 1986, *ApJ*, **307**, 504-534
- Geldzahler B.J., Witzel A., 1981, *AJ* **86**, 1306
- Grandi P., Tagliaferri G., Giommi P., Barr P., Palumbo G. G. C., 1992, *ApJ Supp.* **82**, 93
- Grevesse N., Anders E., 1989, in *Cosmic Abundances of Matter*, AIP 183, ed. C.J. Waddington, New York: American Institute of Physics
- Griffith M. R., Wright A. E., Burke, B. F., Ekers, R. D., 1994, *ApJS* **90**, 179
- Halpern, J. P., 1984, *ApJ* **281**, 90
- Large M.I., Cram L.E., Burgess A.M., 1991, *The Observatory* **111**, 72
- Möller P., Jakobson P., 1987, *ApJ* **320**, L75
- Marscher A. P., 1988, *ApJ* **334**, 552
- Mathur S., 1994, *ApJ* 431, L75
- Mathur S., Wilkes B., Elvis M., Fiore F., *ApJ* 434, 493, 1994
- Morrison R., McCammon D., 1983, *ApJ* **270**, 119
- Otrupcek R., and Wright A. E., 1990, *Proc. Astron. Soc. Austr.* **9**, 170 (PKSCAT90)
- Padovani P., Rafanelli P., 1988, *A&A* 205, 53
- Pan H. C., Stewart G. C., Pounds K. A., 1990, *MNRAS* **242**, 177

- Rinsland C. P., Dixon R. S., Gearhart M. R., and Kraus J. D., 1974, *AJ* **79**, 1129
- Roberts D. H., Burbidge E. M., Burbidge G.R. et al., 1978, *ApJ* **224**, 344
- Sargent W. L. W., Steidel C., Boksenberg A., 1989, *ApJ. Supp.* **69**, 703
- Schartel N., Walter R., Fink H. H., Trümper J., 1996, *A & A*, **307**, 33-51
- Serlemitsos P., Yaqoob T., Ricker G., et al., 1994, *Publ. Astron. Soc. Japan* **46**, L43
- Stark A.A., Gammie C.F., Wilson R.W., et al., 1992, *ApJ Supp.* **79**, 77
- Shull J.M., Van Steenberg M., 1982, *ApJS* **48**, 95
- Wright A. E., Wark, R. M., Troup, E., Otrupcek, R., Jennings, D., Hunt, A., Cooke, D. J., 1991, *MNRAS* **251**, 330
- Weymann R. J., Willems R. E., Peterson B. M., Turnshek D. A., 1979, *ApJ*, **234**, 33
- Weymann R. J., Carswell R. F., Smith M. G., 1981, *Ann. Rev. Astron. Astrophys.* **19**, 41
- Wilkes B. J., Elvis M., Fiore F., et al., 1992, *ApJ* **393**, L1
- Young P., Sargent W.L.W., Boksenberg A., 1982, *ApJ Supp.* **48**, 455